

Computationally efficient model predictive control of freeway networks



Ajith Muralidharan*, Roberto Horowitz

Department of Mechanical Engineering, University of California Berkeley, Berkeley, CA 94720, United States

ARTICLE INFO

Article history:

Received 2 October 2013

Received in revised form 12 January 2015

Accepted 16 March 2015

Available online 15 April 2015

Keywords:

Model predictive control

Optimal control

Ramp metering

Variable speed limits

Computationally efficient controllers

ABSTRACT

A computationally efficient model predictive controller for congestion control in freeway networks is presented in this paper. The controller utilizes a modified Link-Node Cell Transmission Model (LN-CTM) to simulate traffic state trajectories under the effect of ramp metering, variable speed limit control and compute performance objectives. The modified LN-CTM simulates freeway traffic dynamics in the presence of capacity drop and ramp weaving effects. The objective of the controller can be chosen to represent commonly used congestion performance measures like total congestion delay measured in units of vehicle hours. The optimal control formulation based on this modified model is non-convex making it inefficient for direct use within a model predictive framework. Heuristic restrictions and relaxations are presented which allow the computation of the solution using optimal solutions of a sequence of derived linear programs. Mainly, the freeway is cleverly divided into regions, and limited restrictions are placed on solution trajectories to allow us to derive computationally efficient control actions. In the absence of capacity drop, this solution strategy provides optimal solutions to the original optimal control problem by solving a single linear program. The properties of the solution are discussed along with the role of variable speed limits when capacity drop is present/absent. Examples are provided to showcase the computational efficiency of the solution strategy, and scenarios simulated using the modified LN-CTM are analyzed to investigate the role of variable speed limits as a congestion control strategy.

© 2015 Elsevier Ltd. All rights reserved.

1. Introduction

Traffic congestion can be encountered in metropolitan areas during various time periods across the day or sometimes during the night. An average commuter experiences recurrent congestion during his commute due to presence of system bottlenecks. In addition, non-recurrent events, both planned (road work, public events) and unplanned (accidents) contribute increasingly to the unreliability in commute times. The 2012 annual urban mobility report ([David Schrank and Tim, 2012](#)) compiled by the Texas Transportation institute calculated that the average commuter experienced 38 h of delay in 2011, up from 14 h in 1982. In 2011, congestion costs accumulate over \$121 billion dollars, which is more than \$818 per commuter. The easiest way to combat congestion is through infrastructure expansions. Adding additional lanes and new freeways are not always feasible due to economic, environmental or space restrictions. As a result, transportation engineers increasingly rely on intelligent operational management of the existing infrastructure to improve system efficiency, and traffic control is one such strategy.

* Corresponding author.

E-mail addresses: ajith@berkeley.edu (A. Muralidharan), horowitz@berkeley.edu (R. Horowitz).

Ramp metering and variable speed limits are two commonly used control strategies to regulate traffic flow and delay the onset of congestion. Ramp metering is a control method which utilizes a traffic light present at the ramp entrance to regulate the traffic entering the freeway. Over the years, many ramp metering algorithms have been developed and deployed. The simplest ones are fixed time of day controllers which specify a fixed rate at any particular time of the day. Percent occupancy control is a widely deployed traffic responsive ramp metering strategy that uses occupancy thresholds to determine the metering rates. Alinea is a popular ramp metering algorithm based on feedback control theory (Papageorgiou et al., 1991). The basic version is an integral controller, which regulates the density downstream of the ramp to be around the target density (which is usually chosen as the critical density). Compared to the percent occupancy scheme, which is a feed-forward controller, Alinea is a feedback controller and its field implementations have yielded improved performance (Papageorgiou et al., 1997). Various versions of ALINEA, including the upstream ALINEA (which uses density measurements upstream of the ramp) and FL-ALINEA (which uses flow measurements) have been developed (Smaragdis and Papageorgiou, 2003). Various coordinated ramp metering strategies have been presented in literature and deployed in the field. The most popular ones include Compass, Bottleneck algorithm, SWARM (Systemwide adaptive ramp metering), ZONE algorithm and METALINE, among others (Zhang et al., 2001). Heuristic Co-ordinated ramp metering (HERO), a coordinated ramp metering strategy (Papamichail et al., 2010), was recently deployed successfully in the Monash freeway in Australia. Ramp metering is usually deployed in conjunction with queue overrides and integral queue regulators to prevent spill backs from the ramps to the city streets (Sun and Horowitz, 2005).

Recently, variable speed limits(VSL) have captured the interest of researchers and practitioners as another popular control strategy for traffic regulation in freeways. Variable message signs display the current speed limits, often determined in response to the current road, traffic and weather conditions. In some installations, the posted speeds are advisory, while many require mandatory compliance with enforcement. In most of the installations, the main target objective is to ensure traffic safety, and the VSL's are designed to ensure speed reduction and homogenization in locations with high traffic incidents (van den Hoogen and Smulders, 1994). There are a few studies documenting the direct effect of VSL on aggregate traffic flow characteristics (Papageorgiou et al., 2008). Hegyi et al. (2005), Carlson et al. (2010), Carlson et al. (2010), Heydecker and Addison (2011), and Heydecker and Addison (2010) represent a sample of studies that include VSL as one of the components of congestion control.

Model based predictive controllers use predicted demands along with a model of the freeway network to specify ramp metering rates and/or variable speed limits for freeway traffic control. These strategies typically employ an optimal control/optimization framework to design the control actions to minimize a chosen performance objective function (Burger et al., 2013). Historically, simple models have been used to design optimal strategies (Wattleworth, 1965; Blinkin, 1976; Papageorgiou and Mayr, 1982). With improved computational capabilities, more accurate macroscopic models including first order models (eg. Cell Transmission Models, (Daganzo, 1994)) as well as second order models (METANET – Kotsialos and Papageorgiou, 2004) have become popular choices for freeway optimal control formulations in recent years (Kotsialos et al., 2002; Kotsialos and Papageorgiou, 2004; Gomes et al., 2006; Hegyi et al., 2005; Carlson et al., 2010; Papamichail et al., 2010; Carlson et al., 2010). While the formulation of these optimal control problems is typically easy, the challenge remains in specifying a solution technique which can calculate good quality solutions without being computationally intensive. This is because the optimization problems that arise in these optimal control formulations are large-scale in nature (typically involving thousands of variables, at the least, for even a small freeway section), apart from being non-linear and non-convex. Applying commonly available solution techniques lead to large computation times (Kotsialos and Papageorgiou, 2004) with no guarantees of global optimality of the solution. The former proves to be a drawback when the controller is embedded as a part of a model predictive framework, since this requires fast optimizations to be executed repeatedly (Kotsialos and Papageorgiou, 2004). Optimal controller formulations based on second order models like METANET (e.g. Kotsialos and Papageorgiou, 2004; Hegyi et al., 2005; Carlson et al., 2010) suffer from these disadvantages.

In contrast, optimal controller formulations based on the Cell Transmission Model show more promise in terms of computational efficiency and global optimality of the generated solution (Ziliaskopoulos, 2000; Gomes et al., 2006). Gomes et al. (2006) present an optimal ramp metering controller based on the Asymmetric Cell Transmission Model (ACTM) along with an efficient solution strategy. The underlying freeway dynamics in the controller formulation is the ACTM, which is presented as a simplification to the CTM. The motivation for this simplification is to provide a higher quality and efficiently computable solution as compared to the original optimal control problem. The authors presented a relaxed version of this optimal ramp metering problem, and proved that the problems are equivalent in terms of the optimal solution trajectory. The relaxed problem is a linear optimization problem, which can be solved efficiently for large freeway networks with long time horizons. While simplified first order models promise computationally efficient and globally optimal solutions, the underlying models do not incorporate phenomena of interest such as weaving and capacity drops. This limits the usefulness of the solutions in many locations where both these effects may be observed (Papageorgiou et al., 2008).

An optimal controller, which ensures global optimality and fast solutions while accounting for weaving and capacity drop is absent. Therefore, we introduce a new model predictive control strategy based on an augmented Link-Node Cell Transmission Model (LN-CTM) (Muralidharan and Horowitz; Muralidharan, 2012). The model predictive controller solves an optimal control problem at each sample step after measuring the state of the freeway. The modified LN-CTM is used to calculate the state evolution of the freeway in the presence of the capacity drop and ramp weaving effects. The optimal controller constructed using the modified LN-CTM model is shown to be non-convex, and strategies that rely on heuristic assumptions are presented to allow the efficient computation of the solution of the original optimal control problem.

First, the freeway is divided into regions (consisting of a sequence of freeway sections) with only the most downstream section exhibiting capacity drop. Control actions for each region are independently calculated using a non-coordinated (between regions) controller that specifies the ramp metering rates and VSL for all links belonging to the region. Next, carefully designed restrictions placed on solution trajectories using new constraints allow the translation of the original optimization problem for the controller into a relaxed linear program. The optimal solution of the relaxed linear program is then mapped back to provide optimal trajectories and control actions of the restricted optimal control problem. Solution optimality and trajectory properties are also discussed in detail, and it is shown that the formulation provides exact solutions for the original optimal control problem when the capacity drop is absent. Examples of the model predictive controller are presented to demonstrate its application on different scenarios. The role of demand/split ratio predictions as well as effect of control and prediction horizons on controller optimality is explored. This paper extends the results presented by the authors in two conference proceedings (Muralidharan and Horowitz, 2012; Muralidharan et al., 2012) for the modified LN-CTM model with weaving and capacity drop and also provides new theoretical and simulation studies to understand the role of VSL in optimal freeway control.

2. Optimal controller formulation

Ramp metering and variable speed limits are two commonly used control strategies to regulate traffic flow and relieve traffic congestion in freeways. The performance of any controller is primarily judged by its ability to decrease traffic congestion, usually captured by performance metrics like Total Travel Time (TTT), or the Total Congestion Delay (TCD). Given one of these performance functions, optimal control theory allows us to compute the state trajectories as well as the control inputs which minimize the performance objective. Optimal controllers require a state model of the freeway to compute these control laws, and the controller presented here uses the modified LN-CTM as its underlying model. Various parameters used in this section, along with their units are described in [Table 1](#).

2.1. Initial conditions and model parameters

The following parameters and initial conditions must be specified for each link and on-ramp:

- Link i fundamental diagram parameters: Capacity F_i , Free-flow speed V_i and Congestion wave speed W_i .
- On-ramp i parameters (Flow capacity and maximum queue length): C_i , L_i .
- Off-ramp i parameters (Split ratios): $\beta_i(k)$ $k = 1, \dots, K$.
- Initial Conditions: $n_i(0)$, $l_i(0)$ $i = 0, \dots, N$.
- Flow Demands: $Q_i(k)$ $i = 0, \dots, N$, $k = 0, \dots, K$.

Table 1
Model variables and parameters.

Symbol	Name	Unit
F_i	Flow capacity of Link i	veh/period
V_i	Free flow speed of Link i	section/period
W_i	Congestion wave speed of Link i	section/period
n_i^j	Jam density of Link i	veh/section
k	Period number	dimensionless
$v_i(k)$	Speed limit enforced at Link i	section/period
$\beta_i(k)$	Split ratio at node i	dimensionless
$f_i(k)$	Flow out of Link i	veh/period
$n_i(k)$	Number of vehicles (vehicle density) in Link i	veh/period
$s_i(k), r_i(k)$	Off-ramp, on-ramp flow in node i	veh/period
$d_i(k)$	On-ramp i demand	veh/period
$l_i(k)$	Queue length on on-ramp i	veh/period
$r_i^*(k)$	Ramp metering rate for on-ramp i	veh/period
C_i	Flow capacity for on-ramp i	veh/period
L_i	Queue capacity for on-ramp i	veh/period
$Q_i(k)$	Input flow for on-ramp i	veh/period
$Q_0(k)$	Input flow for link 0	veh/period
η_i^f	Weaving coefficient (>1) for flows entering from on-ramp i	dimensionless
η_i^s	Weaving coefficient (>1) for flows exiting through off-ramp i	dimensionless
F_i^{rd}	Reduced flow capacity of link i	veh/period
n_i^{cd}	Density beyond which capacity drop is observed in link i	veh/section
$D_i(k)$	Demand function for Link i	veh/period
$S_i(k)$	Supply function indicating available supply at Link i	veh/period
$R_i(k)$	Total demand from Link i and onramp i to Link $i + 1$	veh/period
I	Set of all sections considered in the model	veh/period
I_d	Sections where a discontinuous capacity drop is considered	

2.2. Modified LN-CTM

The model used in the controller is a modified Link Node Cell Transmission Model (LNCTM), which itself is an extension of the Cell Transmission Model (CTM). This macroscopic model simulates flow and density evolution in the freeway (freeway mainline along with on-ramps; off-ramps are represented as simple sinks, as shown in Fig. 1) in the presence of capacity drops and ramp weaving. Mainline links are modeled as cells while on-ramps and the upstream input links are modeled as simple queues. Each freeway link is specified with a fundamental diagram (Fig. 2) describing its demand and supply functions. The model evolution is described through the density/queue update equations, which are simple conservation equations based on link input and output flows. The flows are calculated by comparing the demands/supply at each freeway junction. [Muralidharan and Horowitz](#) presents a detailed description of the model used here. The model evolution is given by the following equations:

Density update equations : mainline/queue conservation equation

$$\begin{aligned} n_0(k+1) &= n_0(k) + Q_0(k) - f_0(k) \\ n_i(k+1) &= n_i(k) + f_{i-1}(k)(1 - \beta_{i-1}(k)) + r_{i-1}(k) - f_i(k) \quad i = 1, \dots, N \\ l_i(k+1) &= l_i(k) + Q_i(k) - r_i(k) \quad i = 1, \dots, N \end{aligned} \quad (1)$$

Flow equations

$$\begin{aligned} f_N(k) &= D_N(k) \\ f_i(k) &= D_i(k) \times \frac{\min(R_i(k), S_{i+1}(k))}{R_i(k)} \quad i = 0, \dots, N \\ r_i(k) &= \frac{d_i(k)}{\eta_i^r} \times \frac{\min(R_i(k), S_{i+1}(k))}{R_i(k)} \quad i = 1, \dots, N \\ s_i(k) &= f_i(k)\beta_i(k) \quad i = 0, \dots, N \end{aligned}$$

where

$$\begin{aligned} D_i(k) &= \min(n_i(k)v_i(k), \bar{F}_i(k)), \quad \forall i \in I \setminus I_d \\ D_i(k) &= \begin{cases} \min(n_i(k)v_i(k), \bar{F}_i(k)) & \text{if } n_i(k) \leq \max\left(n_i^c, \frac{\bar{F}_i}{v_i(k)(1+(\eta_i^r-1)\beta_i(k))}\right), \\ \frac{\bar{F}_i}{1+(\eta_i^s-1)\beta_i(k)} & \text{otherwise} \end{cases}, \quad i \in I_d \\ \bar{F}_i(k) &= \frac{F_i}{1+(\eta_i^s-1)\beta_i(k)} \quad i = 0, \dots, N \\ R_i(k) &= D_i(k)(1 - \beta_i(k)) + d_i(k), \quad i = 0, \dots, N \\ S_{i+1}(k) &= \min(W_{i+1}(n_{i+1}^l - n_{i+1}(k)), F_{i+1}) \quad i = 0, \dots, N-1 \end{aligned} \quad (2)$$

$$d_i(k) = \eta_i^r \min(r_i^c(k), l_i(k)), \quad 0 \leq r_i^c(k) \leq C_i \quad i = 0, \dots, N \quad (3)$$

I is the set of all freeway links and the set I_d represents the subset of the freeway links that implement the discontinuous capacity drop model. At these locations (bottlenecks caused by lane reductions, for example), flow discharge rate drops from F_i to \bar{F}_i beyond a specified density (n_i^{cd}), consistent with the observations seen in [Chung et al. \(2007\)](#). All on-ramps and off-ramps are associated with weaving factors $\eta_i^r \geq 1$ and $\eta_i^s \geq 1$ respectively and these capture the intensity of lane changes. Weaving at on-ramp merges occur near the on-ramp junctions when vehicles entering the freeway from the ramp execute lane change maneuvers to merge with the freeway traffic. In contrast, weaving near off-ramp diverges actually occur in the link preceding the off-ramp, as vehicles change lanes to leave the freeway. This simple model captures capacity reductions as the intensity of the lane changing behaviors (i.e. values η_i^r and η_i^s) increase, and in both cases a value of 1 indicate the absence of weaving. [Muralidharan and Horowitz](#) presents a detailed description of the properties of the capacity drop and the weaving model. While more complicated models are available (e.g. [Leclercq et al., 2011](#) which models capacity drop as a consequence of merging/acceleration effects, and [Jin \(2010\)](#), where detailed spatial weaving models are introduced), this simple model is chosen for the optimal controller to ensure that efficient solutions can be obtained.

2.3. Objective function

The objective function for the controller needs to directly reflect the level of congestion in the freeway. Total Travel Time (TTT) and Total Congestion Delay (TCD), captured in units of vehicle hours, are good candidate objective functions that capture the aggregate effect of traffic congestion on all users in the freeway. For our optimal controller, we define the following generalized linear objective function, based on the macroscopic variables defined in our model.

$$J = \sum_{k=1}^K \sum_{i=0}^N (n_i(k) + l_i(k) - \alpha_i(k)f_i(k) - \bar{\alpha}_i(k)r_i(k)) \quad (4)$$

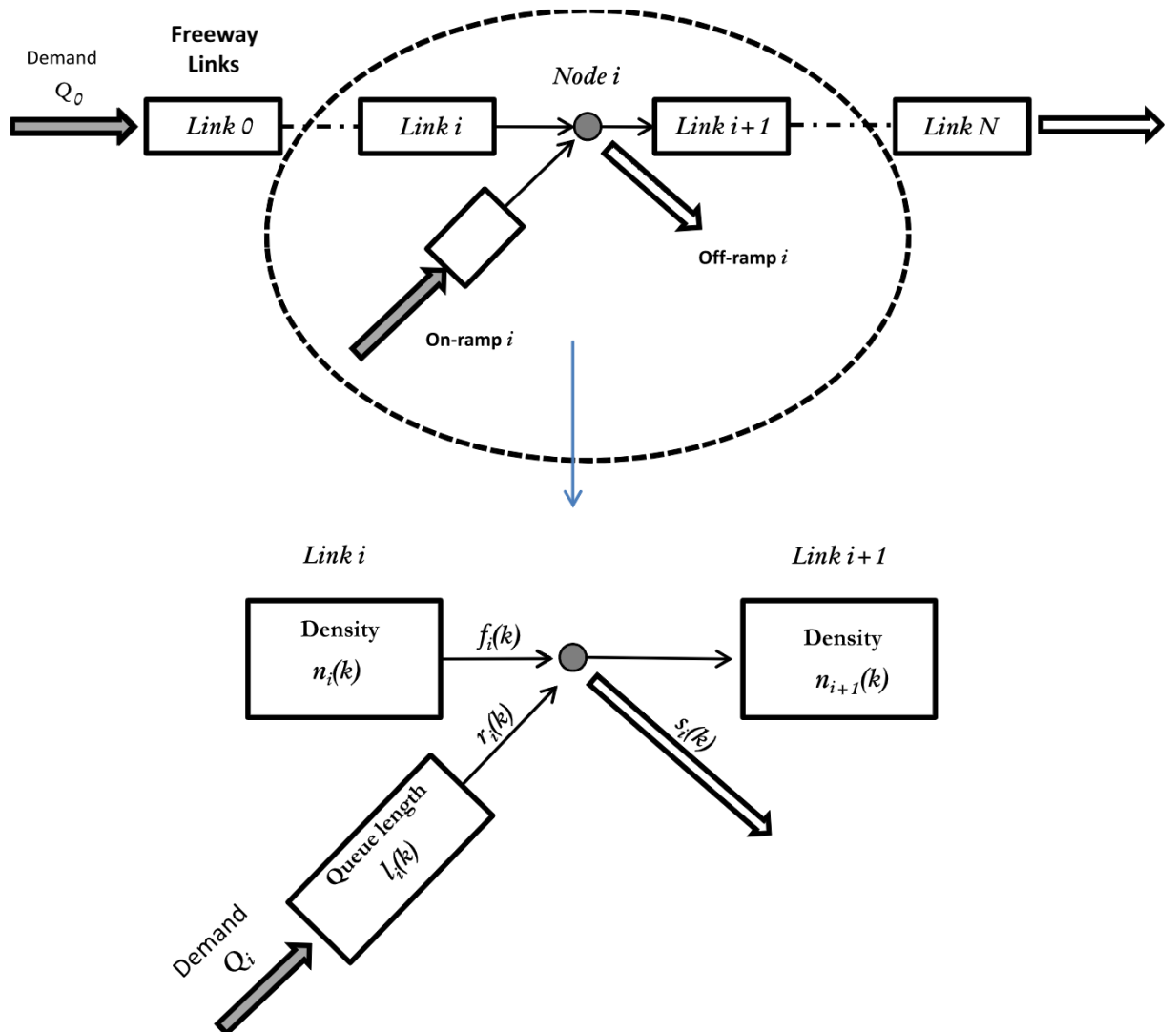


Fig. 1. Freeway with $N + 1$ links. Each Node contains a maximum of one on- and one off-ramp. Note that Node i is downstream of Link i .

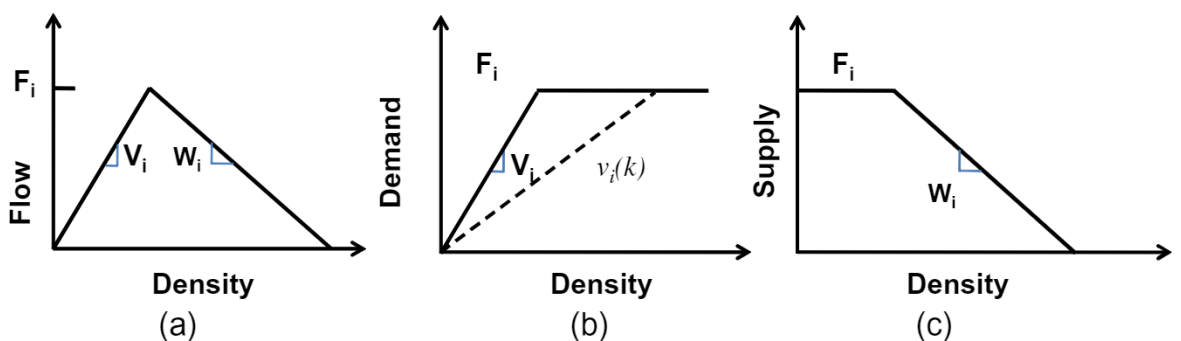


Fig. 2. Triangular fundamental diagram, and demand/supply functions.

where $k = 1 \dots K$ denotes the time period and $i = 0 \dots N$ denotes the link ($n_i(k)$) or ramp ($l_i(k)$) index. By choosing values for the parameters $\alpha_i(k) \geq 0$, $\bar{\alpha}_i(k) \geq 0$, we can represent the following commonly used objective functions.

$$\begin{aligned} J_a &= TTT = \sum_{k,i} (n_i(k) + l_i(k)) \quad \text{Total Travel Time} \\ J_b &= TCD = \sum_{k,i} \left(n_i(k) + l_i(k) - \frac{1}{V_i} f_i(k) \right) \quad \text{Total Congestion Delay} \end{aligned} \quad (5)$$

2.4. Control mechanisms and additional constraints

The optimal controller regulates the traffic using a speed limit profile $v_i(k)$ and a time varying ramp metering rate $r_i^c(k)$. The speed limit profile serves as an indirect control mechanism for regulating flows that exit any particular link of the freeway to enter into the next downstream section. Ramp metering rate serves to regulate the flow entering into the freeway through any particular ramp by storing additional vehicles in the ramps. Natural restrictions on these variables are captured by the following constraints.

$$0 \leq v_i(k) \leq V_i, \quad 0 \leq r_i^c(k) \leq C_i \quad (6)$$

The variable speed limit controller is allowed to impose time varying speed limits up to the maximum speed limit of the freeway section. The ramp metering controller specifies any realizable flow rate up to the maximum flow capacity of the ramp C_i . Zero ramp metering rates ($r_i^c(k)$) can be specified by our controller. In practice, many agencies require a minimum ramp metering rate to ensure that vehicles waiting in ramp queues get serviced without excessive delay. However, having no restrictions on the lower bound for the ramp metering rates will be useful to ensure the validity of the solutions proposed in the next section. Some indirect methods can be used to implement a minimum ramp metering rate and these are described in [Muralidharan and Horowitz](#). To ensure that queues not exceed available storage and affect arterial traffic, we also introduce the maximum queue constraint

$$l_i(k) \leq L_i \quad (7)$$

2.5. Optimal control formulation

Combining the objective functions, the freeway dynamic model and the constraints, the final problem can be written as

$$\min : J, \text{ given by Eq. (4)}$$

$$S.t. : \text{For } k = 1, \dots, K$$

$$\text{Conservation and flow equations : Eqs. (1)–(3)}$$

$$\text{Constraint equations : Eqs. (6) and (7)}$$

$$n_i(k), l_i(k), f_i(k), r_i(k) \geq 0 \quad \forall i$$

$$\text{initial conditions/fundamental diagram parameters given in Section 2.1.}$$

$$(8)$$

In the formulation above, the objective (Eq. (4)), conservation equations (Eq. (1)), constraint equations (Eqs. (6)) are all linear functions of flow and density variables. Flow equations (Eqs. [\(2\)](#) and [\(3\)](#)) contribute to the non-linearity of the optimal control problem. In the next section, we discuss assumptions and approximations that allow us to solve the optimal controller problem efficiently. Finally, for optimal control of a freeway network, it is customary to present a single controller to control the entire freeway network. However in some cases (including the solution strategy discussed in the next section) it might be advantageous to divide the freeway into regions, and implement an independent controller for each. In that case, the same formulation can be used to represent the optimal controller for the particular region.

3. Computationally efficient controllers

The methodology presented in this section to derive a computationally efficient model predictive controller builds on the approach presented in [Muralidharan and Horowitz \(2012\)](#) and [Muralidharan et al. \(2012\)](#). The controller formulated in the previous section [\(2.5\)](#) involves non-linear optimization, with no guarantees for global optimality. Even when the problem is formulated for a modest time horizon (say 15 min), the optimization problem usually involves tens of thousands of variables which contribute to computational inefficiency. There are two sources of non-linearity introduced in our formulation (Eqs. [\(2\)](#) and [\(3\)](#)): (a) A discontinuous non-linearity introduced through the capacity drop equations and (b) a continuous (but non-differentiable) non-linearity introduced through the flow update equations, which involves the ramp flows, mainline flows along with the speed limit profiles and the ramp metering rates. The approach presented below introduces assumptions and relaxations that allow us to derive the optimal control actions and state trajectories by solving an equivalent linear optimization problem.

To develop a computationally efficient controller, first we employ a “divide and conquer” approach. This approach is motivated by some of the observations presented in [Gomes et al. \(2008\)](#), which analyzes the set of equilibrium points

corresponding to known stationary, feasible ramp demands. All equilibrium points can be described by dividing the freeway into the same regions (which consists of multiple links), where the first link is in free-flow while the last link is a bottleneck discharging at its maximum flow capacity. The set of equilibrium points capture varying levels of congestion, but there is always one equilibrium which corresponds to the freeway in free-flow. The role of an optimal controller would be to steer the freeway to this optimal point, possibly from another equilibrium point (which shares the same boundary flow conditions), and this could be achieved by deploying an independent (non-coordinated) region-wise controller which only controls links within the region. Under time-varying demands, we can expect that these bottleneck regions could possibly change as bottleneck regions merge and new bottleneck regions are created. While in theory, every latent bottleneck can be triggered by available demands, a few of these bottlenecks are recurrent. If we observe traffic contours over multiple days, we usually find that a small number of these bottleneck locations are triggered frequently (Chen et al., 2004 presents an automatic bottleneck identification algorithm which can be used to locate these), even under the presence of time varying demands. For example, the presence of the capacity drop at lane merges generally creates a natural recurrent bottleneck.

To employ our approach, we separate the freeway into non-overlapping regions, with each region consisting of only one bottleneck with a modified demand function at its most downstream link. Note that inside each region, we may have multiple latent/active bottlenecks as long as they do not experience capacity drops. A controller based on an optimal control framework will be described for each region, where the controller will prescribe ramp metering rates and speed limits for all links belonging to the section. The complete control of the entire freeway will be managed by independent controllers each of which act on one region. In this section, we will describe the process of solving the optimal control problem for each of these sections. We capture this using the following assumption.

Assumption 3.0.1. Each freeway region considered has only one bottleneck described using the modified demand function. This bottleneck with the capacity drop will be located in the most downstream section, ie. link N .

It is expected that the bottleneck locations usually experience free-flow conditions downstream. However, congestion from another downstream bottleneck location can also impact the downstream boundary. First, we will develop our predictive controller under the assumption that the location downstream of the bottleneck is in free-flow. Later, the controller will be modified to account for congestion downstream.

3.1. Problem simplification

We now define two optimal control problems. **Problem Q** is a restricted non-linear optimal control problem for our individual region, which reduces the problem to a mixed integer program. **Problem R** solves **Problem Q** through a sequence of relaxed linear programs.

First, we introduce a new binary variable $\mu(k) \in \{0, 1\}$, $\forall k$, to capture the “mode” of the final link. This “mode” can either correspond to free-flow or capacity drop, depending on whether link density is less/greater than n_N^{cd} . The constraints that replace the modified demand function are

$$\begin{aligned} D_N(k) &= \min(n_N(k)v_N(k), F_N + (\bar{F}_N - F_N)\mu(k)) \\ n_N(k) &\leq n_N^{cd}(1 - \mu(k)) + \eta_N^r\mu(k) \\ n_N(k) &\geq n_N^{cd}\mu(k) \\ \mu(k) &\in \{0, 1\} \end{aligned} \quad (9)$$

For the equations above, the feasible values of $\mu(k)$ map to

$$\begin{aligned} \mu(k) = 0 &\iff n_N(k) \leq n_N^{cd}, \quad D_N(k) = \min(n_N(k)v_N(k), F_N) \\ \mu(k) = 1 &\iff n_N(k) \geq n_N^{cd}, \quad D_N(k) = \min(n_N(k)v_N(k), \bar{F}_N) \end{aligned} \quad (10)$$

Given $n_N(k)$, the feasible solutions satisfying the new constraints are equivalent to the original definition of the modified demand functions at all points except when $n_N(k) = n_{cd}^N$, since the demand function can either take on the value F_N or \bar{F}_N when the density exactly equals n_{cd}^N . However, in the definition of the demand function with the capacity drop, there is a discontinuity at this operation point, and the demand function takes on the value F_N at this density. Even though the constraints are not an exact representation of this discontinuous demand function, the solution of the **Problem Q** will force the demand function to take the value F_N at $n_N(k) = n_N^{cd}$. An intuitive explanation for this fact is to realize that we can decrease the performance objective by maximizing the output flow at the final link.

Next, we absorb the ramp metering variables ($r_i^c(k)$) by relaxing the problem. Eqs (6) and (3) can be replaced by $0 \leq d_i(k) \leq \eta_i^r \min(C_i, l_i(k))$ and the optimal ramp metering profile can be obtained by choosing $r_i^c(k) = d_i(k)/\eta_i^r$. This is only possible since the lower bound of the ramp metering rate is set to 0. Finally, we introduce the following assumption in **Problem Q**.

Assumption 3.1.1. For the freeway section considered, we restrict the system evolution such that once the downstream link switches to the “free-flow” mode, it remains in the free-flow mode.

This heuristic restriction is expected to produce an optimal cost almost similar to the original optimal control problem, since the free-flow mode is more efficient as it allows vehicles to exit the region at a much faster rate. Hence, once the system switches into the free-flow mode, it is usually optimal for the controller to maintain this mode for maximum throughput. Using this assumption we get,

Problem Q Modified Problem

$$\begin{aligned}
 \min : & J, \text{ given by Eq. (4)} \\
 \text{s.t. :} & \text{For } k = 1, \dots, K \\
 & \underline{\text{Conservation and flow equations}} : \text{Eqs. (1) and (2) with (9) replacing the modified demand function} \\
 & \underline{\text{Constraint equations}} : \\
 & 0 \leq v_i(k) \leq V_i \\
 & 0 \leq d_i(k) \leq \eta_i^r \min(C_i, l_i(k)) \\
 & l_i(k) \leq L_i \\
 & n_i(k), l_i(k), f_i(k), r_i(k) \geq 0 \\
 & \mu(k) \geq \mu(k+1) \quad k = 1, \dots, N-1 \\
 & \mu(k) \in \{0, 1\} \quad k = 1, \dots, K \\
 & \text{with given initial conditions/parameters.}
 \end{aligned} \tag{11}$$

In the above formulation, the feasible region of $\mu(k)$ can also be expressed as follows,

$$\mu(k) \geq \mu(k+1) \quad k = 1, \dots, K-1 \iff \exists j \in \{1 \dots K\} \text{ s.t. } \mu(k) = 1, \quad k = 1, \dots, j, \quad \mu(k) = 0, \quad k = j+1, \dots, K \tag{12}$$

This interpretation is used to formulate **Problem R**. For a given j , we formulate an equivalent linear program by relaxing the flow constraints. We convert the non-linear equality constraints in the flow equations to a set of linear inequality constraints, by absorbing the control variables $v_i(k)$ and $d_i(k)$. The final optimal control problem solves a linear program for each j and uses the minimum cost solution to obtain the optimal trajectory.

Problem R Final Problem

$$\min_{j=0 \dots K} J_j^*,$$

where

$$\begin{aligned}
 J_j^* = \min & J, \text{ given by Eq. (4)} \\
 \text{s.t.} & \text{For } k = 1, \dots, K
 \end{aligned}$$

Conservation equations : Eq. (1)

Relaxed flow equations :

$$\begin{aligned}
 \bar{f}_i(k) &\leq \bar{n}_i(k)V_i \quad i = 1, \dots, N \\
 \bar{f}_i(k)(1 + (\eta_i^s - 1)\beta_i(k)) &\leq F_i \quad i = 1, \dots, N \\
 \bar{f}_i(k)(1 - \beta_i(k)) + \eta_i^r \bar{r}_i(k) &\leq F_{i+1} \quad i = 1, \dots, N-1 \\
 \bar{f}_i(k)(1 - \beta_i(k)) + \eta_i^r \bar{r}_i(k) &\leq W_{i+1}(n_{i+1}^l - \bar{n}_{i+1}(k)) \quad i = 1, \dots, N-1
 \end{aligned}$$

Constraint equations :

$$0 \leq \bar{r}_i(k) \leq \min(C_i, \bar{l}_i(k)) \quad i = 1, \dots, N$$

$$\bar{l}_i(k) \leq L_i$$

$$\text{For } k = 1, \dots, j$$

$$\bar{n}_N(k) \geq n_N^{cd}$$

$$\bar{f}_N(k)(1 + (\eta_N^s - 1)\beta_N(k)) \leq \bar{F}_i$$

$$\text{For } k = j+1, \dots, K$$

$$\bar{n}_N(k) \leq n_N^{cd}$$

$$n_i(k), l_i(k), f_i(k), r_i(k) \geq 0 \quad i = 1 \dots N$$

$$\text{with the same initial conditions/parameters.}$$

(13)

An upper bar is added to the optimization variables in each subproblem of **Problem R** (e.g. $\bar{n}_i(k)$, $\bar{f}_i(k)$, $\bar{r}_i(k)$) in order to distinguish them from their counterparts in **Problem Q**. The main differences between the two problems is that we do not explicitly consider the link velocity variables ($v_i(k)$) and the on-ramp demands ($d_i(k)$) in **Problem Q**. This formulation is

derived by expanding the feasible set to include all possible trajectories with different feasible realizations of the control variables. Next, we will outline the methodology adopted to convert a solution of **Problem R** to a solution of **Problem Q**.

3.2. Solution

Each subproblem of **Problem R** is a linear program. The j th subproblem captures the situation when the system is in the capacity drop mode for the first j time instants and thereafter switches to the free-flow mode. Depending on the initial conditions, some of these subproblems may be infeasible. Let $j^* = \operatorname{argmin}_{j=0 \dots K} J_j^*$, denote the subproblem that produces the optimal cost. We denote the corresponding optimal trajectory as $\bar{n}_i^*(k)$, $\bar{f}_i^*(k)$, $\bar{l}_i^*(k)$, $\bar{r}_i^*(k)$. This is converted into an optimal control/solution trajectory $(n_i^*(k), f_i^*(k), l_i^*(k), r_i^*(k), v_i^*(k), d_i^*(k))$ for **Problem P|Q** using the conversion algorithm given below.

Algorithm 1. Conversion algorithm A

For each time period k and link $0 \leq i \leq N$,

$$n_i^*(k) = \bar{n}_i^*(k)$$

$$f_i^*(k) = \bar{f}_i^*(k)$$

$$l_i^*(k) = \bar{l}_i^*(k)$$

$$r_i^*(k) = \bar{r}_i^*(k)$$

$$\tilde{F}_i^*(k) = \frac{F_i}{1 + (\eta_i^s - 1)\beta_i(k)}$$

For each time period k and link $0 \leq i < N - 1$,

$$\text{if } f_i^*(k) = \min(n_i^*(k)V_i, \tilde{F}_i^*(k))$$

$$v_i^*(k) = V_i$$

$$d_i^*(k) = \eta_i^r r_i^*(k)$$

otherwise if $f_i^*(k)(1 - \beta_i(k)) + \eta_i^r r_i^*(k) < S_{i+1}^*(k)$

$$v_i^*(k) = f_i^*(k)/\eta_i^r$$

$$d_i^*(k) = r_i^*(k)\eta_i^r$$

$$\text{otherwise if } \frac{r_i^*(k)\eta_i^r}{S_{i+1}^*(k)} \leq \frac{\min(C_i, l_i(k))\eta_i^r}{\min(n_i^*(k)V_i, \tilde{F}_i^*(k))(1 - \beta_i(k)) + \eta_i^r \min(C_i, l_i(k))}$$

$$v_i^*(k) = V_i$$

$$d_i^*(k) = \eta_i^r r_i^*(k) \times \frac{\min(n_i^*(k)V_i, \tilde{F}_i^*(k))(1 - \beta_i(k))}{S_{i+1}^*(k) - \eta_i^r r_i^*(k)}$$

otherwise

$$v_i^*(k) = \frac{\eta_i^r \min(C_i, l_i(k))}{n_i^*(k)(1 - \beta_i(k))} \times \left(\frac{S_{i+1}^*(k)}{\eta_i^r r_i^*(k)} - 1 \right)$$

$$d_i^*(k) = \eta_i^r \min(C_i, l_i(k))$$

$$\text{where } S_i^*(k) = \min(W_i(n_i^l - \bar{n}_i^*(k)), F_i(k))$$

and for each time period k

$$\tilde{F}_N(k) = \begin{cases} \frac{F_N}{(1 + (\eta_N^s - 1)\beta_N(k))} & \text{if } n_N(k) \leq n_N^{cd} \\ \frac{\bar{F}_N}{(1 + (\eta_N^s - 1)\beta_N(k))} & \text{otherwise} \end{cases},$$

$$\text{if } f_N^*(k) = \min(n_N^*(k)V_N, \tilde{F}_N)$$

$$v_N^*(k) = V_N$$

else

$$v_N^*(k) = f_N^*(k)/n_N^*(k)$$

$$\mu^*(k) = 1, \quad 1 \leq k \leq j^* \quad \text{and} \quad \mu^*(k) = 0 \quad \text{o.w}$$

(14)

From the solution trajectory derived above, the speed limit variables can be directly applied as the control input, while the on-ramp demands are used to obtain the ramp metering rates $r_i^c(k) = d_i(k)/\eta_i^r$.

3.3. Equivalence of solutions

In this section, we show that the solution derived using the algorithm above is optimal for **Problem Q**.

Lemma 3.3.1. Let $Q := \{n_i(k), f_i(k), l_i(k), r_i(k), v_i(k), d_i(k), \mu(k)\}$ be the solution derived from $R := \{\bar{n}_i(k), \bar{f}_i(k), \bar{l}_i(k), \bar{r}_i(k), j^*\}$ using **Conversion algorithm A**. Then Q is a feasible solution for **Problem Q** if R is a feasible solution of **Problem R**. Q and R evaluate to identical costs for the respective optimization problems.

Lemma 3.3.2. Let $Q = \{n_i(k), f_i(k), l_i(k), r_i(k), d_i(k), v_i(k), \mu(k)\}$ be a feasible solution of **Problem Q**, then the projected solution $R = \{n_i(k), f_i(k), l_i(k), r_i(k)\}$ is a feasible solution for subproblem j in **Problem R**, where j is the index where $\mu(j) = 0$, $\mu(j-1) = 1$. Moreover, Q and R evaluate to identical costs for the respective optimization problems.

The proofs for the lemmas above are presented in [Muralidharan and Horowitz](#). They will be used to prove the main theorem, stated below.

Theorem 3.3.1. Let $R = \{\bar{n}_i^*(k), \bar{f}_i^*(k), \bar{l}_i^*(k), \bar{r}_i^*(k)\}$ be an optimal solution of **Problem R** and $Q = \{n_i^*(k), f_i^*(k), l_i^*(k), r_i^*(k), v_i^*(k), d_i^*(k)\}$ be the solution derived using **Conversion algorithm A**. Then Q is an optimal solution for **Problem Q**.

Proof 1. [Lemma 3.3.1](#) shows that Q is a feasible solution for **Problem Q**. Suppose Q is not optimal for **Problem Q**, i.e. there is another solution Q' which evaluates to a lower cost. [Lemma 3.3.2](#) allows us to compute a new solution R' which is feasible for **Problem R**, and also has a lower cost than R (which has a cost equivalent to Q). This contradicts the fact that R is optimal for **Problem R**. Thus Q , derived from R is an optimal solution of **Problem Q**. \square

When [Assumption 3.1.1](#) is valid, this solution is also optimal for the original optimal control problem for the given region.

3.4. Downstream congestion

When the downstream boundary is congested, we make the following assumption,

Assumption 3.4.1. For the freeway section considered, the downstream boundary condition can be represented using a constant boundary flow restriction F^d .

The boundary flow restriction means that flows from the most downstream location cannot exceed F^d . Under free-flow conditions we have $F^d = F_N$, but as the link downstream of our downstream boundary begins to get congested, it restricts the flow that can exit the region and $F^d < F_N$. The downstream flow restriction is assumed to be constant, even though the downstream flow restriction will be usually time varying and dependent on the upstream flows. However, with our model predictive control strategy, we will use the current downstream flow measurement to provide an estimate of F^d . This is updated to a better estimate during the next controller update step.

When $F_N \geq F^d > \bar{F}$, we can replace F_N by F^d , and solve the optimal control problem as before. In this case, even when $F_N > F^d$, free-flow mode in the first link increases the current section throughput. However, when $\bar{F}_N > F^d$ this is no longer true, since both modes are equally efficient with respect to maximizing discharge from the particular section. In fact, in this case, it is efficient to switch to the congested mode, since this allows the freeway section to store more vehicles (due to the increased density prevalent in the capacity drop mode) thereby releasing some of the congestion upstream. This leads to larger exit flows in the blocked off-ramps. We set $F_N = F^d$ and solve the following single linear program to obtain the optimal solution in this case.

$$\min J, \text{ given by Eq. (4)}$$

$$\text{s.t. For } k = 1, \dots, K$$

Conservation equations

[Eq. \(1\)](#)

Relaxed flow equations

$$\bar{f}_i(k) \leq \bar{n}_i(k)V_i \quad i = 1, \dots, N$$

$$\bar{f}_i(k)(1 + (\eta_N^s - 1)\beta_N(k)) \leq F_i \quad i = 1, \dots, N$$

$$\bar{f}_i(k)(1 - \beta_i(k)) + \eta_i^r \bar{r}_i(k) \leq F_{i+1} \quad i = 1, \dots, N-1$$

$$\bar{f}_i(k)(1 - \beta_i(k)) + \eta_i^r \bar{r}_i(k) \leq W_{i+1}(n_{i+1}^l - \bar{n}_{i+1}(k)) \quad i = 1, \dots, N-1$$

Constraint equations

$$\begin{aligned} 0 &\leq \bar{r}_i(k) \leq \min(C_i, \bar{l}_i(k)) \quad i = 1, \dots, N \\ \bar{l}_i(k) &\leq L_i \\ n_i(k), l_i(k), f_i(k), r_i(k) &\geq 0 \quad i = 1 \dots N \\ \text{with the same initial conditions/parameters.} \end{aligned} \tag{15}$$

The problem shown above does not explicitly track the mode of the most downstream condition, since the downstream flows are limited by the downstream boundary flow restriction. The optimal solution of the above linear program can be used to obtain speed limit profiles and ramp metering rates using **Conversion Algorithm A**, with a slight modification. We need to replace the calculations for determining the speed limit profile in the last section by

$$v_N^*(k) = \begin{cases} V_N & \text{if } f_N^*(k) = \min\left(n_N^*(k)V_N, \frac{F_N}{(1+(\eta_N^*-1)\beta_N(k))}\right) \\ f_N^*(k)/n_N^*(k) & \text{o.w.} \end{cases} \tag{16}$$

Generally, the optimal controller does not specify a restrictive speed limit profile for the last link in any of the cases mentioned above, as these would increase the delay of vehicles in the freeway region considered. This can also be shown rigorously.

The results derived above can be extended in the following scenarios.

1. Hard queue constraints are substituted by soft queue constraints, which are beneficial to maintain solution feasibility during MPC.
2. Zero ramp metering rates are discouraged, to promote user equity.
3. Constraints on average waiting time need to be included.
4. Smooth speed limit changes are desired in the solution trajectory.

Details about these modifications are presented in [Muralidharan and Horowitz](#).

3.5. Remarks

In the problem formulation, we have also allowed the split ratio, $\beta_i(k)$ to be time-varying. However, one needs to be careful while searching for an optimal speed control profile in the case of time-varying split ratios. For example, consider the case where the split ratios for the first cell increase with time. In this case, an optimal speed control law might initially hold back vehicles (by decreasing the speed limit), so that the vehicles catch a higher split ratio, and exit the freeway. This does not reflect reality, since the vehicles are routed to the wrong destination. This effect is exacerbated when J_a is considered as the objective, since vehicles that exit do not contribute to the Total Travel Time in the downstream links. In contrast, augmenting the objective with the flow terms ($-f_i(k)$) serves to alleviate this effect here, as vehicles exiting the freeway do not contribute to the flow downstream. In the case of decreasing split ratios, the roles of these terms are reversed. Hence we argue that J_b or J_c is a better objective function to consider for the problem. In the case of constant split ratios, this problem does not arise. This problem is not unique to a optimal control formulation using the LN-CTM, but arises due to the use of a split-ratio based routing scheme adopted by this model. This observation was hinted by the authors in [Gomes et al. \(2006\)](#).

Also, the solution methodology presented introduces different assumptions to tackle the presence of the capacity drop. In the case when the capacity drop is not present, the entire freeway can be controlled by a single optimal controller. Moreover, the original optimal control problem can be solved exactly using the relaxation procedure given above. In fact, **Problem R** reduces to a single linear program, and this leads to a very efficient solution strategy. In fact, under this formulation, duality can be exploited to answer questions related to severity of bottlenecks, plan ramp capacity expansions etc.

3.6. Characteristics of the solution and role of VSL

In this section, we explore the characteristics of the solution of the optimal control problem, in the case of constant split ratios. The presence of the capacity drop in the model necessitates the use of variable speed limits. In this section, we will show that these speed limits serve two purposes (a) Throttling of the flow into the link with the capacity drop (b) facilitating optimal merging which may be useful to maintain queue limits on the on-ramps. The following theorem is useful for that purposes. Without loss of generality, we assume that only the most downstream section experiences capacity drop.

Theorem 3.6.1. *When the optimal trajectory satisfies $\eta_i^* \bar{r}_i(k) < \min(F_{i+1}, W_{i+1}(n_{i-1}^l - \bar{n}_{i+1}(k)))$, $\forall k$ and $i = 1 \dots N - 2$, the following are true,*

1. The constraint $\bar{f}_i(k) \geq 0$ is never active, and
2. Atleast one of the following constraints are active.

$$\begin{aligned}\bar{f}_i(k) &\leq \bar{n}_i(k)V_i \\ \bar{f}_i(k) &\leq \frac{F_i}{(1 + (\eta_i^s - 1)\beta_i(k))} \\ \bar{f}_i(k)(1 - \beta_i(k)) + \eta_i^r\bar{r}_i(k) &\leq F_{i+1} \\ \bar{f}_i(k)(1 - \beta_i(k)) + \eta_i^r\bar{r}_i(k) &\leq W_{i+1}(n_{i+1}^l - \bar{n}_{i+1}(k))\end{aligned}$$

In [Muralidharan and Horowitz](#), a proof based on KKT conditions is provided. As seen above, the theorem applies to all links which are not upstream of a link with a modified capacity drop function. It shows that when the optimal controller specifies a speed limit for any link discharging its output to a “normal” link (i.e. without a capacity drop), the optimal controller does not throttle the flow by means of a speed limit, i.e.

$$f_i(k) = \min \left(\bar{n}_i(k)V_i, \tilde{F}_i, \frac{\min(F_{i+1}, W_{i+1}(n_{i+1}^l - \bar{n}_{i+1}(k))) - \eta_i^r\bar{r}_i(k)}{1 - \beta_i} \right)$$

When the downstream link has no ramp flows, we see that outflow in the optimal solution follows the LN-CTM equations with nominal speed limits. Also, even in the presence of capacity reduction due to weaving, the speed limits do not throttle the flow reaching the downstream intersection. However, when the ramp has non-zero flow and the downstream link is congested (i.e. the third term in the equation stated before is active), a speed limit may still be applied to ensure optimal merging. Even in this case, the total inflow into the next link will be the same as the flow in the no speed limit case, but in the case of the optimal trajectory the total outflow may be arbitrarily divided between the ramp and the previous link. In some cases, this will correspond to the application of a speed limit. For example, when ramp flows satisfy the third conditional statements in **Conversion Algorithm A**, speed limits are not necessary, while speed limits need to be specified when the fourth conditional statement is active. The most common reason for this is that in cases when queue limits are specified, in order to maintain the queue within its limit, the controller will try to assign more preference to the ramp flow, by means of reduced speed limits to the link.

The theorem above is violated in cases of extreme congestion/excessive ramp demands and limited queue storage, where $\bar{r}_i(k) < W_{i+1}(n_{i+1}^l - \bar{n}_{i+1}(k))$ may not apply and the optimal controller might lead to additional throttling to ensure that sufficient space is available for ramp demand. This condition is not violated when $\eta_i^rC_i < W_{i+1}(n_{i+1}^l - \bar{n}_{i+1}(k))$ for the optimal trajectories. During nominal operation, freeways do not generally get very congested as to violate this condition. We also expect the same when the freeway is under the effect of the optimal controller. Finally, the theorem does not apply for the link feeding into the section which experiences a capacity drop. In this segment, as we will see in the examples in the next section, speed limits are used to throttle the flow allowing the possibility that none of the upper bound constraints is active during some periods in the optimal trajectory. It is interesting that solution characteristic is consistent with the observations in [Carlson et al. \(2010\)](#) which employs second order models for speed limit control. The authors postulate that near optimal solutions could be obtained by applying variable speed limits only at a location slightly upstream of the capacity drop (taking into account an acceleration segment, which corresponds to the length of Link i in our case). In our case, the VSL is only applied one link upstream (at the upstream boundary of the bottleneck link) which is Len_i miles upstream of the bottleneck location.

4. Evaluation

In this section, we present examples involving the application of a model predictive controller (MPC). The model predictive controller solves an open loop optimal control problem online based on the modified LN-CTM model at each sampling time, using the state information measured at the current sampling time, which include the densities n_i and the onramp queues l_i . The controller implements the control steps of the obtained optimal control profile till the next sampling time, and then the process is repeated ([Borrelli et al.](#)).

Let T and N_p denote the model time step and prediction horizon (in units of time periods) used in the optimization problem respectively. We execute the MPC every N_c time periods, which corresponds to $T_c = N_c \times T$ time instants (here we assume that N_p, N_c are natural numbers). We refer to this period N_c as the controller execution horizon. At the sampling time period, we calculate the controller actions for the next N_p time steps, but apply the control actions for the next N_c time periods before repeating the process at the next sampling period. The split ratio is assumed to be constant, equal to the split ratio observed at the instant the controller is initiated. This averts the problem related to time varying split ratios detailed previously, and does not usually lead to any appreciable decrease in the controller performance within the MPC framework. We also adopt soft constraints for queues and use total congestion delay, as the controller optimization cost.

We demonstrate the controller performance using two sets of examples. In the first case, we consider a synthetically constructed network, with artificial demands. The examples demonstrate the application of the controller in the presence of weaving and capacity drop. In the second set of examples, we demonstrate the application of the controller on a calibrated

model of the I-80E freeway route (Muralidharan, 2012) between the Bay Bridge and the Carquinez Bridge in the Bay area. The calibrated model did not indicate capacity drops at any location. All the simulations are performed using the modified LN-CTM model.

4.1. Example set 1: Artificial example

We demonstrate the application of our controller in the presence of weaving and capacity drop. Fig. 3 represents the geometry of the freeway Section (3.2 mile length) which is considered for our simulation studies. The geometry is artificially constructed to demonstrate the application of our controllers. In this portion of the freeway, link 11 is the only link which experiences a capacity drop. The fundamental diagram parameters are listed in Table 2. We can see that the maximum throughput of link 11 is 7600 vph in free-flow conditions. This decreases to 7300 vph once the density in link 11 exceeds the critical density of 121 vpm. This represents a capacity drop of around 4% which is representative of the nominal capacity drop generally reported in literature. We assign our optimal controller to operate on links 0–11. The optimal controller can specify variable speed limits for these links, in addition to the ramp metering rates for the on-ramps 1–3. A constant split factor $\beta = 0.15$ is chosen for the three off-ramps during the entire time period considered. For all the on-ramps, we assume a weaving ratio $\eta_r = 1.3$. We do not consider any off-ramp weaving in the examples shown here. Fig. 4 shows the on-ramp demands we use for the simulation. The on-ramp demands are chosen such that the freeway is congested between the times 1 h and 2 h. We use a constant flow of 7000 vph as the input flow into the first link on the freeway (link 0). We use the LN-CTM with the capacity drop/weaving model to perform our simulations.

4.1.1. Freeflow downstream conditions

In the first simulation, we assume that the boundary downstream of link 13 is in free-flow. Fig. 5(top) shows the velocity contours that result when no control action is applied. We can see two bottlenecks in the simulation, at link 3 and link 11 respectively. The bottleneck in link 11 is attributed to the capacity drop, while the bottleneck in link 3 is due to the on-ramp merge and weaving (this bottleneck disappears when weaving factor equals 1 for the demands in the simulation example).

Next, we simulate the freeway, with the model predictive controller specifying the metering rates and speed limits. The controller is initially turned off to allow congestion to build up and we start applying the controller at time 1.11 h, when link 11 already experiences capacity drop. We choose $N_p = 30$, $T = 10$ s, $N_c = 6$ for our controller. The queue limits in both the ramps are chosen to be 75 vehicles. We choose ΔV_i (Muralidharan and Horowitz) to correspond to 5 mph to limit the variations in speed in the link preceding the bottleneck section. In this case, the controller has to solve at most 30 (and in most cases, less) linear programs.

Fig. 5(middle), shows results of the simulation in which our model predictive controller is used. In this case, the severity and the extent of congestion is reduced. Fig. 5(bottom) shows the variable speed limit profiles specified by our optimal

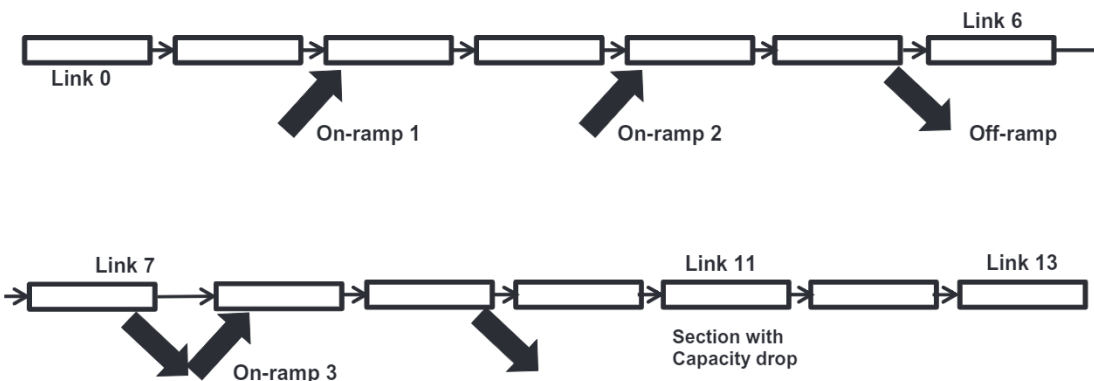


Fig. 3. Freeway geometry with location of on-ramps and off-ramps.

Table 2

Link parameters, commonly reported units.

Links	V^*	W^*	F^* (vph)	\bar{F}^*
0, 1	65 mph (104.61 kph)	20 mph (32.19 kph)	8500	n.a
2, 3	65 mph (104.61 kph)	20 mph (32.19 kph)	8900	n.a
4–10	65 mph (104.61 kph)	20 mph (32.19 kph)	10,500	n.a
11	65 mph (104.61 kph)	20 mph (32.19 kph)	7900	7300 vph
12, 13	65 mph (104.61 kph)	20 mph (32.19 kph)	7600	n.a

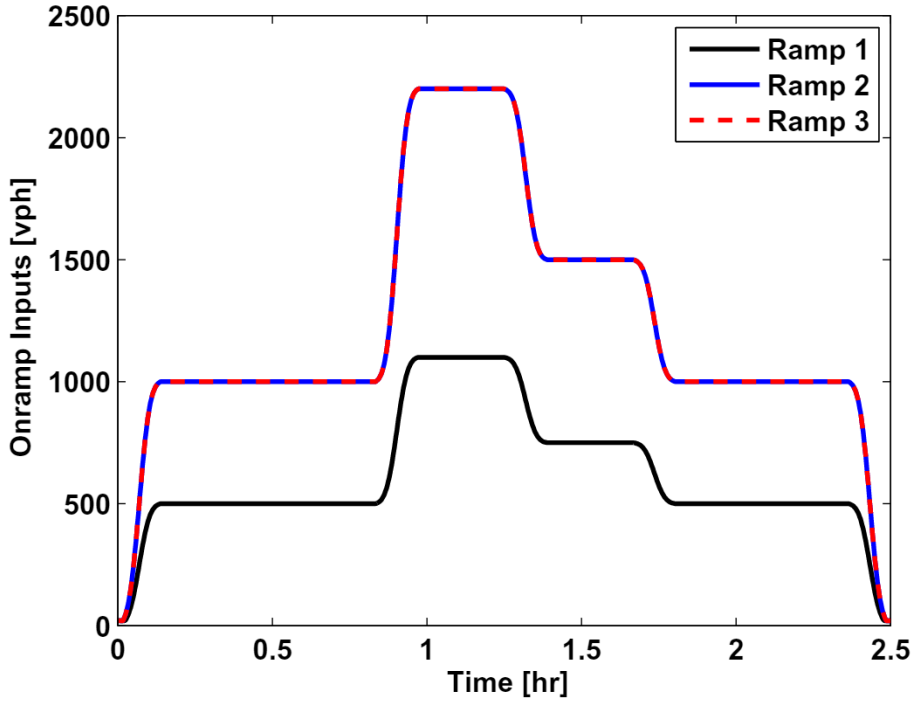


Fig. 4. On-ramp input flows for all ramps. Note: On-ramps 2 and 3 have the same flows.

controller. The optimal controller specifies a speed limit profile for link 10, and this helps decrease the density of link 11 to a value below its critical density. Thereafter, it still maintains the speed limit which enables link 11 to stay in free-flow. Thus, the optimal controller creates a new bottleneck, through controlled congestion, at link 10 to prevent link 11 from experiencing a drop in capacity. This controlled congestion helps in increasing the throughput of link 11, which limits the extent of congestion, even though it is not completely eliminated. Finally, we see from Fig. 6 that the optimal controller maintains the ramp queue limits. The most downstream ramp meter corresponding to on-ramp 3 is used to control the congestion arising out of the bottleneck at link 10. In contrast, the flows in on-ramp 2 are controlled to alleviate the effects of weaving. The operational capacity at node 3 is decreased in presence of weaving, and this is proportional to the on-ramp flows. Therefore, at this ramp, decreasing the on-ramp flows (until queue constraints are violated) temporarily increases the operational capacity of the section, which increases the discharge out of the section and reduces total delay. For every additional vehicle stored in the on-ramp, $\eta_r = 1.3$ vehicles are discharged from the previous section, since weaving vehicles occupy space equivalent to 1.3 vehicles. In cases when the congestion spills back to block other off-ramps upstream of the current ramp, this increase in operational capacity can further help delay congestion.

The total travel time and the delay experienced by all users in the no-control scenario are 1358 vh (vehicle-hours) and 245 vh respectively. In contrast, these reduce to 1256 vh and 143 vh respectively when the controller is used. This leads to a substantial delay reduction of 41.5%.

4.1.2. Congested downstream conditions

In the second simulation, the boundary downstream of link 13 is initially in free-flow. At 1.4 h, the boundary (link 13) begins to get congested and this congestion propagates back onto link 11 soon after. At 1.6 h, the boundary becomes free-flowing. All other parameters and demands are same as the first simulation.

Fig. 7(top) shows the velocity contours under the no-control scenario. The congestion is more widespread as compared to the simulation with the optimal controller (Fig. 7(middle)). In this simulation, the controller utilizes the solution methodology specified in Section 3.4. From Fig. 7(bottom), we note the speed limit profiles specified by the controller. In this case, we see that the controller specifies a speed limit profile until the boundary congestion reaches the location downstream of link 11. Congested boundary conditions result in $\bar{F}_N > F^d$, and in this scenario, the optimal controller no longer specifies a restrictive speed limit for the link feeding into the capacity drop section. Once the downstream congestion dissipates, the predictive controller resumes the speed limit control to maximize the throughput.

The total travel time and the delay experienced by all users in the no-control scenario are 1364 vh and 252 vh respectively. In contrast, these reduce to 1284 vh and 172 vh respectively when the controller is applied. This leads to a delay reduction of 31.8%.

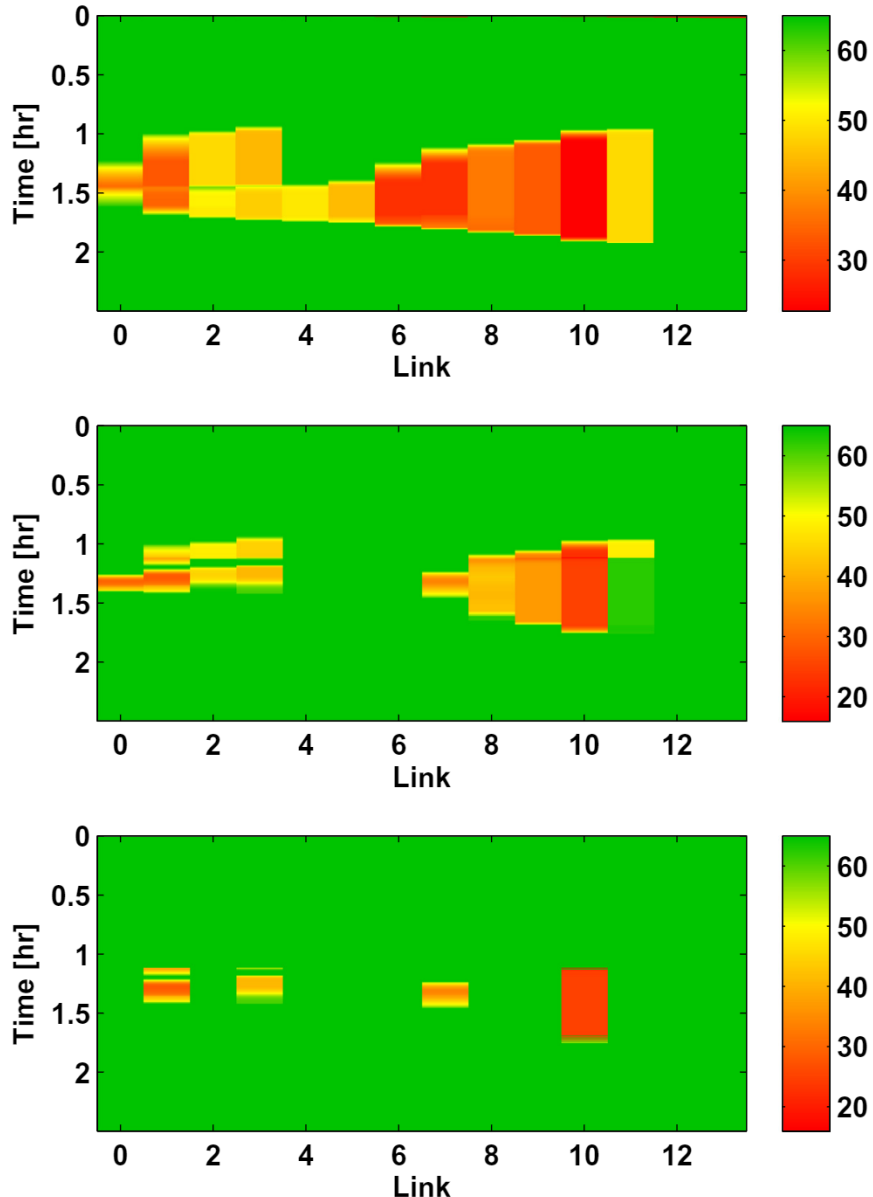


Fig. 5. Top: Simulated Velocity contours [mph] – no control scenario. Middle: Simulated Velocity contours [mph] – optimal controller. Bottom: Optimal speed limit profile [mph].

4.2. Example set 2: Calibrated I-80E model

For the next set of examples, we use a calibrated model of the I-80E freeway in the Bay area between the Bay Bridge and the Carquinez Bridge. The model consists of 34 links connecting to 28 onramps and 27 offramps. The model was calibrated (the calibration process is described in [Muralidharan \(2012\)](#) and [Muralidharan et al. \(2009\)](#)) to replicate the congestion patterns observed on September 2nd, 2008. [Fig. 8](#)(Top) shows the speed contours produced by the model without any control measures activated. This freeway experiences congestion during the evening commute periods, and we limit the temporal axis to cover the evening congestion. The calibration procedure did not locate significant capacity drop at any section. Thus, the entire freeway is controlled using a single model predictive controller, and the solution can be obtained by solving a single linear program.

We apply a model predictive controller with $T = 10$ s, $N_p = 100$ and $N_c = 9$ to specify the ramp metering rates and speed limit profile for this freeway. A queue limit of 50 vehicles was imposed for all the ramps. The actual demand profiles were assumed to be known and used to specify the demands in the controller. Constant split ratios, equal to the split ratios at the

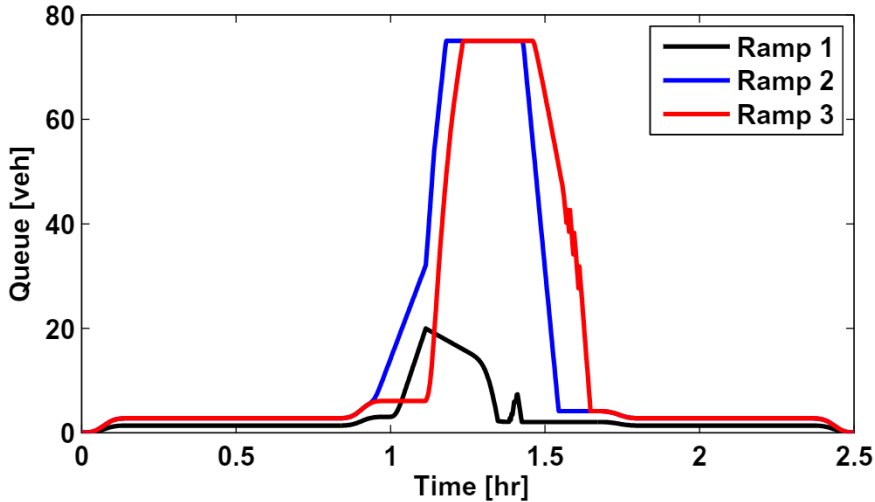


Fig. 6. On-ramp queues for simulation 1 with optimal controller. Each ramp has a maximum queue size of 75veh.

time period of controller actuation, were used. Fig. 8(middle) represents the speed contour observed when the MPC is used, and Fig. 8(bottom) shows the speed limit profile generated by the MPC. Given the limited queue size constraint imposed on the controller, the controller did not completely eliminate the congestion present in the freeway. However, the MPC succeeds in delaying the onset of congestion on the freeway. In this scenario, the controller resulted in a delay reduction of 17.85%. In Fig. 9, we show the resulting queues on all the onramps. We see that the queue constraints are not adversely violated in this case (when $C = 5$ was chosen), as the queue lengths are within the 50 veh/ramp limit.

4.2.1. Role of quality of demand and split ratio estimates

Next, we explore the role of perfect demand and split ratio information on the performance gains obtained using the MPC, as seen in Table 3. We choose the demand/split ratio information to either be exact (ie. equal to the actual realized profiles in the simulation model), or constant (equal to the realized value at the instant the controller is initiated). We caution that the delay reduction with exact split ratios (with/without exact demands) are just shown for comparison. In this case, the optimal controller decreased the speeds to very low values during some periods, so that vehicles can exit the freeway at a later time, when the split ratio values are higher, and this does not simulate a realistic scenario. Nonetheless, this study shows that we can expect a marginal decrease in delay reduction when operating with constant splits. The effect of not knowing the exact demand information also leads to a small decrease in the performance gains. We have observed that the controller performance is more sensitive to the inaccuracy of demand information around the start time of the prediction horizon. For example, if incorrect demand information is provided for the first N_c steps, we observed a marked decrease in the controller performance. In contrast, decrease in accuracy of the demands along the prediction horizon does not affect the controller performance, as long as the demand information around the current time periods is accurate. In this case, when the MPC is executed during the next time period, we get more accurate demands to recalculate the future control actions. In fact, when constant demands (equal to the realized value at the instant the controller is initiated) are chosen, the demand information around the controller actuation period is quite accurate, since our demand profiles are sufficiently smooth. We also explore the effect of various parameters on the performance of the model predictive controller. In these parametric studies, we use exact demands and constant split ratios. Table 4 lists the performance of the MPC when the controller execution horizon, prediction horizon and the maximum queue limit, are varied. We have generally observed that the controller execution horizon is more critical than the prediction horizon. In particular, we note that prediction horizons can be as short as 10 min ($N_p = 60$) in this case. The prediction horizon is dependent on freeway size, and this can be decreased for shorter freeway sections. In contrast, we see that the controller execution horizon needs to be sufficiently small i.e 2 or 3 min ($N_c \approx 12 - 18$). Longer controller execution horizons lead to a decrease in controller performance (this was found to be the case irrespective of the prediction horizon chosen). The main reason for the need for shorter controller horizons is the use of constant split ratios in our models. In the case of imperfect demand information, controller execution horizons further determine the performance of the controller, as short control execution horizons allow the controller to correct the demand estimates used inside the MPC, as well as measure the queues and indirectly account for the faulty ramp demand estimates. We observed a performance decrease of 2% as we changed the N_c from 6 to 18, when constant demands and constant split ratios were used. Short N_c values necessitate the use of a fast optimization routine in the MPC. Finally, we also see that ramp queues limits have a major effect on the efficiency gains that can be expected out of the controlled system.

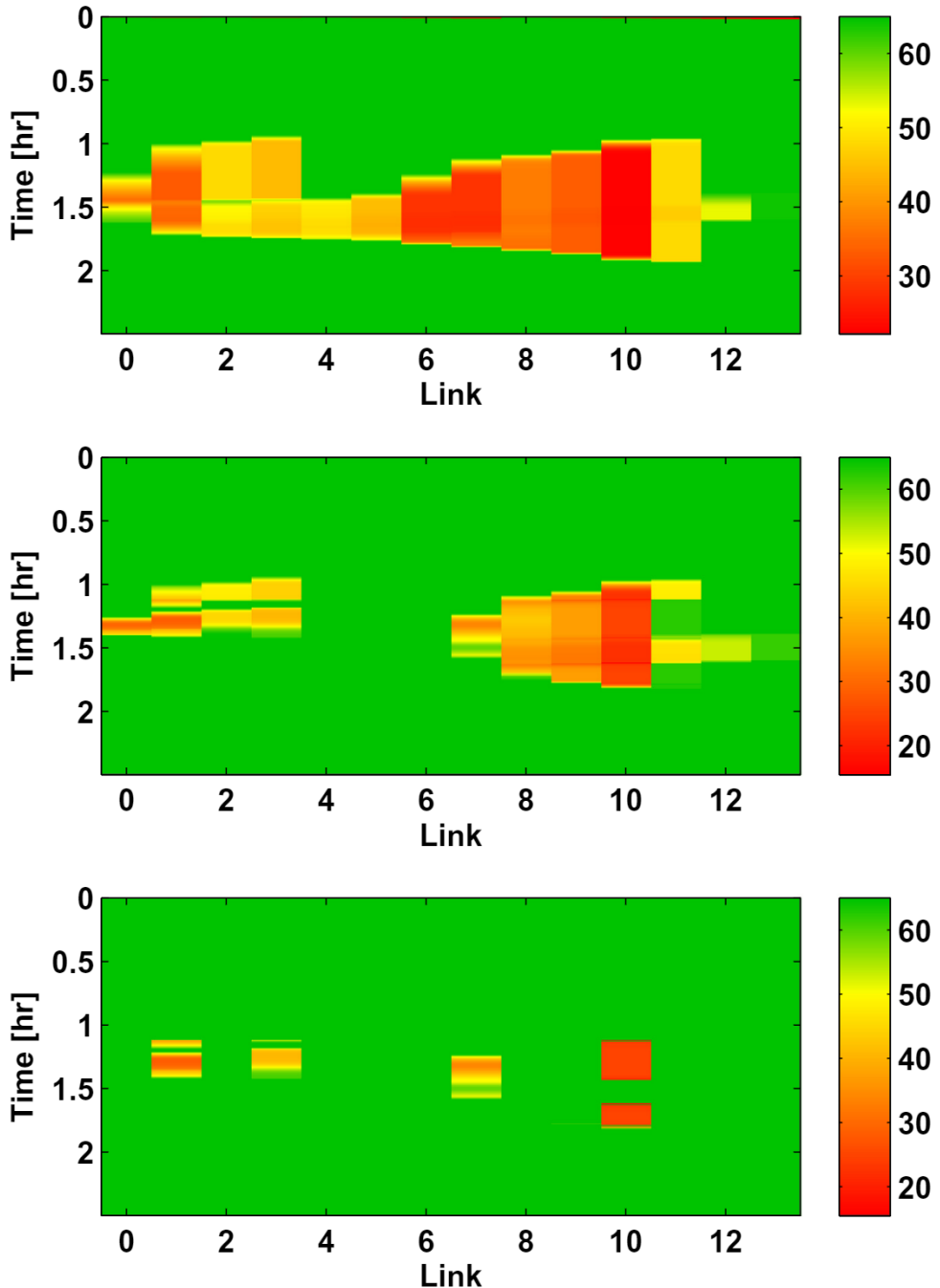


Fig. 7. Top: Simulated Velocity contours [mph] – no control scenario. Middle: Simulated Velocity contours [mph] – optimal controller. Bottom. Optimal speed limit profile [mph].

4.2.2. Role of VSL in optimality of solution

Finally, we explore the role of variable speed limits in the optimal control formulation when the capacity drop is absent. In the scenario demonstrated in the first experiment in the second set, variable speed limits are important to ensure that ramp queue limits are not violated. Generally, when the link downstream of a ramp starts getting congested, the controller meters the ramp flows entering into the section, and the on-ramp queues build up. However, once the queue reaches its limit, the optimal controller needs to maintain the ramp flow to be equal to the demand entering the ramp, so that queues do not exceed the given limits. When the link downstream gets congested, and the demand from the upstream freeway mainline is also high, these ramp flow rates cannot be realized only by specifying high ramp metering rates (this corresponds

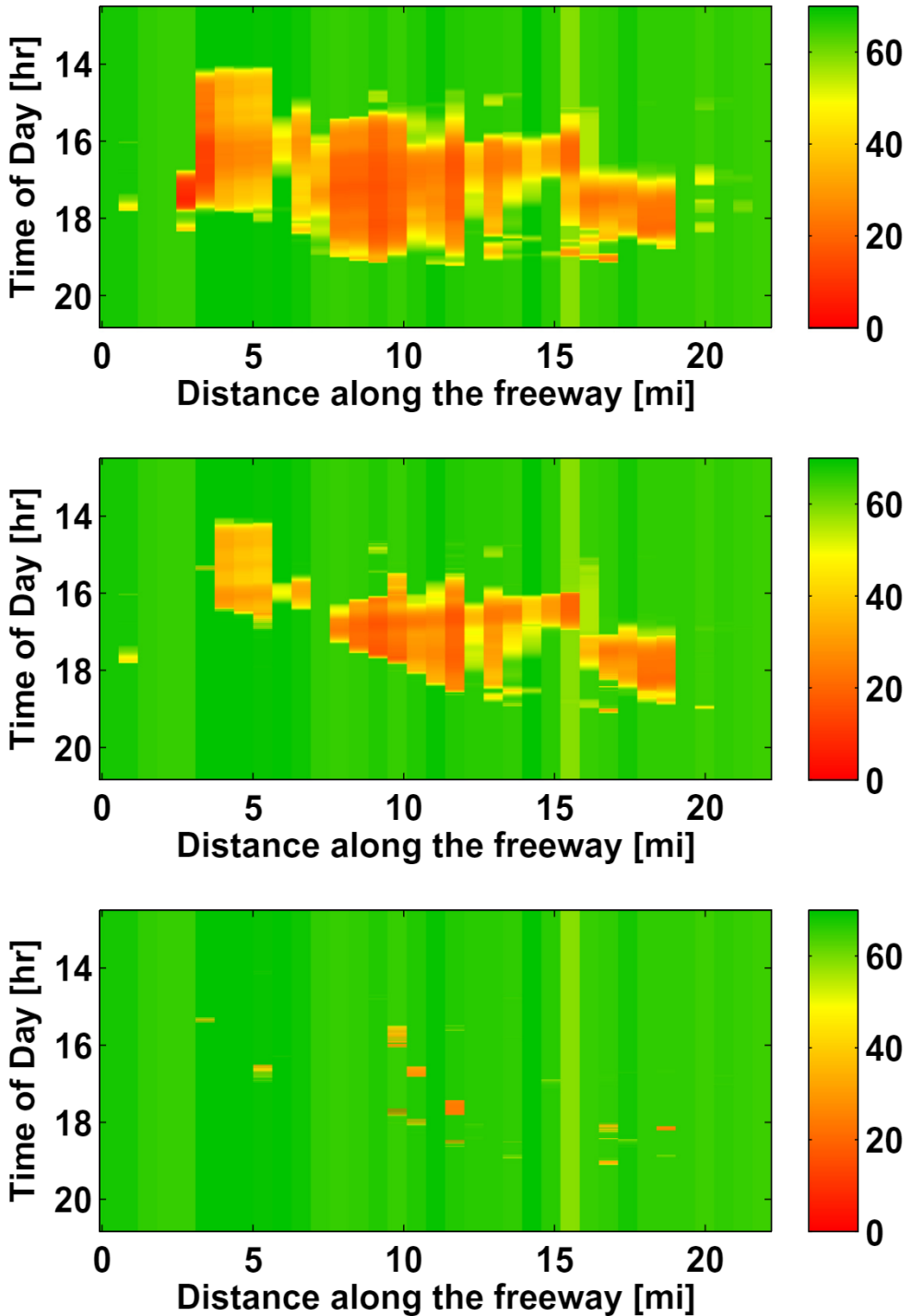


Fig. 8. Top: Speed contours in the uncontrolled case. Middle: Speed contours with ramp metering and VSL. Bottom: VSL specified by the MPC.

to the fourth conditional statement in **Conversion algorithm A**). Variable speed limits help maintain the queue limits in this case. We carried out a simulation experiment (with the same parameters as the first experiment explained above), where we only applied the ramp metering portion of the control actions specified by the MPC, while discarding the variable speed limits. This resulted in a delay reduction of 17.78%, which is very similar to the performance gains in the first simulation. However, the queues in some of the on-ramps were violated, as seen in Fig. 10. When ramp queue limits were not used, discarding the VSL and applying the ramp metering portion of the control actions lead to a performance gain of 25.26%, as

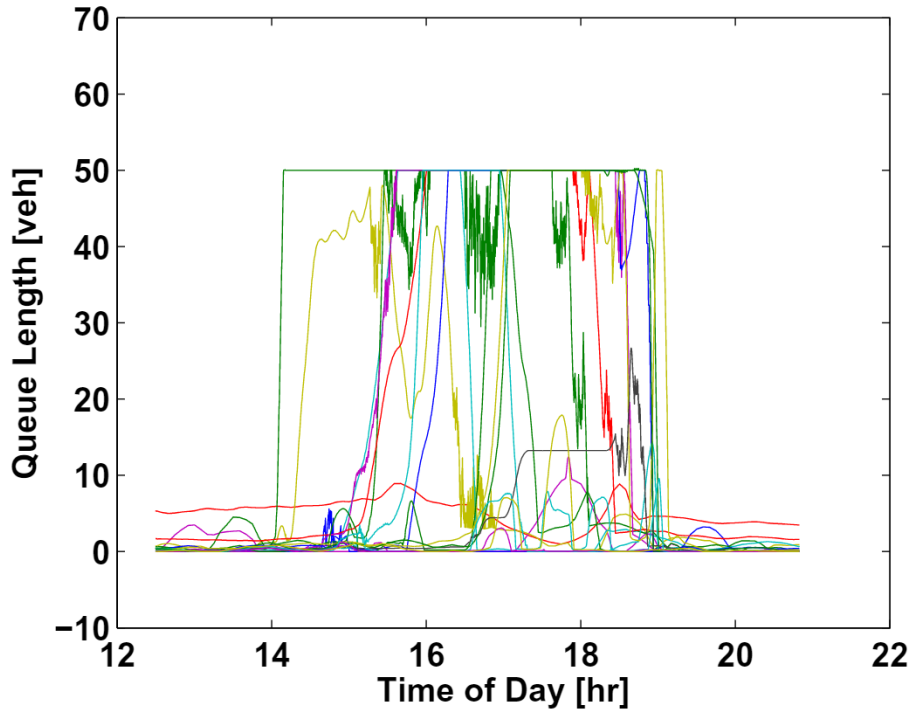


Fig. 9. Queue lengths in the controlled case.

Table 3
Role of demand and split ratio information.

Demands	Split ratio	Delay reduction (%)
Exact	Exact	18.85
Constant	Exact	18.28
Exact	Constant	17.85
Constant	Constant	17.42

Table 4
MPC parameter study.

N_c ($N_p = 120, L_i = 50$)	6	12	18	~4	30
Delay reduction (%)	17.91	17.76	17.55	17.2	15.96
$N_p, N_c = \alpha, L_i = 50$	30	60	90	120	150
Delay reduction (%)	17.82	17.85	17.85	17.85	17.85
$L_i(N_p = 120, N_c = 9)$	10	20	50	100	∞
Delay reduction (%)	7.6	11.7	17.86	23.8	25.65

compared to the delay reduction of 25.34%, when the complete controller was used. It is our conjecture that variable speed limits do not contribute to significant performance improvements for the freeways in the absence of capacity drop, if maintaining exact queue limits are not a priority.

4.2.3. A note on computational speed

A 2.4Ghz Intel Core 2 Duo laptop with 4 GB of RAM was used to compute the solutions presented in this section. In the scenarios corresponding to the first set of examples, each control step involved solving multiple linear programs each with around 2000 variables, 700 equality and 5000 inequality constraints. Each step was solved within 5 s using the MOSEK linear program solver ([Mosek](#)). We also see that our sequence of linear programs can be solved completely in parallel, which would further decrease the solver time. For example set 2, which contained a large freeway network covering 23 miles, when $N_p = 100$, $T = 10$ s and $n = 33$ the solution was obtained by solving a single linear program with approximately 17,000

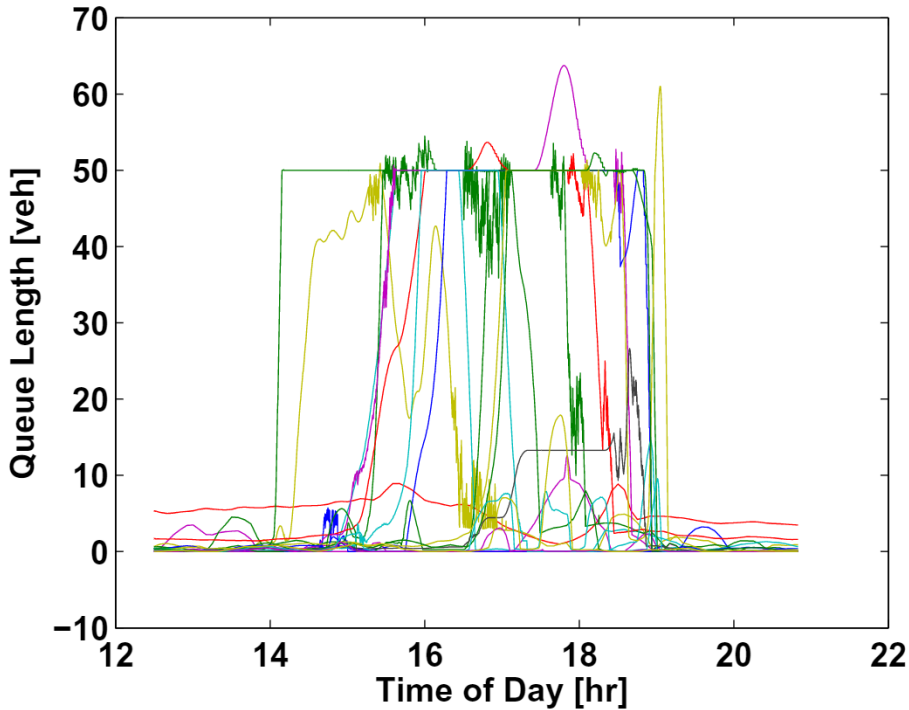


Fig. 10. Queue lengths, when only the ramp metering portion of the optimal controller is used.

variables, 35,000 inequality and 7000 equality constraints. MOSEK solved each iteration within 1 s. Even when the capacity drop model is introduced for a freeway of this size (which would involve solving 100 linear programs for each control step), we can exploit the parallelism to compute the solution efficiently. We also expect that an intelligent strategy could be designed to limit the number of linear programs solved at each step, if required.

4.2.4. A note on solution robustness

The simulations shown in this section assume that the freeway dynamics can be described by the modified LN-CTM model, and that the parameters are exactly known. While a full study of the robustness (and solution strategies to improve it) are beyond the scope of this paper, we present some notes on the expected performance of the system under different types of uncertainty. The example set 1 with freeflow boundary conditions is used to present the results.

First, we found that the controller is robust under varying levels of uncertainty for the ramp weaving factors. Particularly, when the example scenario was simulated with $\pm 5\%$ random perturbations to the ramp demands functions (which translate to an uncertainty in weaving functions), the performance objective was near optimal, producing almost 41.3% reduction in delay. In addition, if $\pm 5\%$ random perturbations are added to the ramp flow inputs, the performance only drops by a modest 0.05%. However, the controller is not robust to mainline flow errors near the capacity drop section. $\pm 2.5\%$ random perturbations were added to the supply function and this reduced the delay reduction to 19.5%. When the controller time period was reduced from 5 to 1 simulation timestep, the delay reduction was 31%. This was due to the fact that the feedback controller can partially compensate for model errors. However, the controller is not able to completely compensate the model errors, because the errors can prevent the freeway section from switching out of the capacity drop mode. When the model errors were only applied to all sections except the sections neighboring the capacity drop section, and the controller time step is set to be equal to the simulation time step, the performance improvements were near optimal levels, leading to a reduction of delay of 41.5%.

The results presented above, in the presence of random flow uncertainties, are not surprising. It is expected that even robust PID controllers, tuned to maintain flows near critical density, would perform poorly in this scenario. The main reason for the poor performance is the presence of a discontinuous capacity drop. When a controller (including our optimal controller) maintains the density of the capacity drop section near the critical density, any random perturbations can move the density above the critical capacity, leading to a capacity drop. In this scenario, a controller needs to be tuned to maintain a margin of robustness (i.e. regulate the density to values below a fixed margin from the critical density), and this margin could be estimated in real time. Our optimal controller can be easily modified to reflect this by adding a soft constraint reflecting the required margin, and the resulting controller is expected to be robust.

5. Conclusion and comments

We presented a model predictive control approach based on a modified LN-CTM to specify ramp metering rates and variable speed limits in a freeway. The modified LN-CTM model simulates freeway dynamics in the presence of capacity drop and ramp weaving along with the effects of ramp metering and variable speed limits. Since the underlying optimal control problem used in the model predictive controller involves non-linear, non-convex and discontinuous constraints, we identify limited assumptions that are needed to allow us to solve it efficiently. First, we divide the freeway into regions and assume that each region is controlled using an independent controller which controls all sections within that region. One drawback to this approach is that we cannot completely co-ordinate all controller actions, and this might limit the total performance improvements in some cases. When the downstream boundary of each region always remains in free-flow, lack of co-ordination should not impact controller performance; however, during periods when the region boundary transitions into congestion, better co-ordination may help manage and delay its propagation. Next, we also assume that the optimal trajectory does not switch back from the free-flow mode to the capacity drop mode. Again, when the downstream boundary is always in free-flow, this assumption is generally valid, since the free-flow mode is generally more efficient in discharging traffic out of the region. Finally, we assume that congestion in the downstream boundary can be represented by a constant flow capacity restriction for flows exiting the final link. This provides us a tractable method to calculate a predictive control strategy when the downstream boundary is congested. All these assumptions allow us to specify an efficient predictive controller used when sections of the freeway exhibit capacity drop. When capacity drop is absent (or negligible) these assumptions are not necessary, and we can solve the original optimal control problem exactly. In fact, the solution can be obtained by solving a single linear program in this case.

We presented different simulation examples, highlighting the controller performance in scenarios with/without capacity drops. We also presented some analysis and simulation results to investigate the characteristics of the optimal solution, with respect to the role of variable speed limits within our controller. Variable speed limits are useful in two cases: (a) to ensure optimal merging in on-ramp junctions and (b) to limit the feeding flows into the section that experiences capacity drop. VSL application corresponding to (a) is generally useful in maintaining queue limits, as we had demonstrated with Example set 2. The performance gains with the application of VSL in this case may be limited, as shown by our simulations where we only applied the ramp metering portion of the controller. In contrast, VSL specified in case (b) is necessary to increase the efficiency of the capacity drop section. We expect that an optimal controller that only uses ramp metering to prevent capacity drop might be more inefficient and less robust.

We also demonstrated the feasibility of deploying this strategy for real time model predictive control. It was seen that controller sampling period N_c should be at least 30 s to ensure good quality solutions in the absence of perfect predictions. The solution strategy was also shown to be computationally efficient, as all solutions were obtained well within the controller sampling time restriction of 30 s, without using specialized hardware. We also presented preliminary results on the robustness of the controller in the presence of random perturbation errors. The results showed that the controller is robust to most errors except for errors in the flows (captured by errors in the supply functions) near the capacity drop section. The optimal controller could be modified in this scenario to improve the robustness.

The model controller, used on a calibrated model, allows us to get an estimate of the best performance benefits that can be obtained by implementing ramp metering and variable speed limits in the field. For freeways without capacity drop, this estimate is quite accurate since we obtain a globally optimal solution to the optimal control problem. These estimates are invaluable to compare, certify and possibly tune other commonly deployed ramp metering and variable speed limit controllers. Being computationally efficient, this controller can also be possibly deployed in the field in the future.

Acknowledgements

This work is supported by National Science foundation CDI Grant 0941326. The contents of this paper reflect the views of the authors and not necessarily the official views or policy of the National Science Foundation. The authors are grateful for various discussions with the TOPL group, and particularly to Prof. Pravin Varaiya and Dr. Gabriel Gomes for their invaluable feedback and comments.

Appendix A. Supplementary material

Supplementary data associated with this article can be found, in the online version, at <http://dx.doi.org/10.1016/j.trc.2015.03.029>.

References

- Blinkin, M., 1976. Problem of optimal control of traffic flow on highways. *Automat. Control* 37 (3), 662–667.
- Borrelli, F., Bemporad, A., Morari, M., 2012. Predictive Control. <<http://www.mpc.berkeley.edu/mpc-course-material>> (accessed 01.2012).
- Burger, M., van den Berg, M., Hegyi, A., Schutter, B.D., Hellendoorn, J., 2013. Considerations for model-based traffic control. *Transp. Res. Part C: Emerg. Technol.* 35 (0), 1–19, doi:<http://dx.doi.org/10.1016/j.trc.2013.05.01>. <<http://www.sciencedirect.com/science/article/pii/S0968090X13001125>>.
- Carlson, R.C., Papamichail, I., Papageorgiou, M., Messmer, A., 2010. Optimal motorway traffic flow control involving variable speed limits and ramp metering. *Transp. Sci.* 44 (2), 238–253.

- Carlson, R.C., Papamichail, I., Papageorgiou, M., Messmer, A., 2010. Optimal mainstream traffic flow control of large-scale motorway networks. *Transp. Res. Part C: Emerg. Technol.* 18 (2), 193–212. <http://dx.doi.org/10.1016/j.trc.2009.05.014>, <<http://www.sciencedirect.com/science/article/pii/S0968090X09000771>>.
- Chen, C., Skabardonis, A., Varaiya, P., 2004. Systematic identification of freeway bottlenecks. *Transp. Res. Rec.* 1867, 46–52.
- Chung, K., Rudjanakanoknad, J., Cassidy, M.J., 2007. Relation between traffic density and capacity drop at three freeway bottlenecks. *Transp. Res. Part B: Methodol.* 41 (1), 82–95. <http://dx.doi.org/10.1016/j.trb.2006.02.011>, JURL <http://www.sciencedirect.com/science/article/pii/S0191261506000397>.
- Daganzo, C., 1994. The cell transmission model: a dynamic representation of highway traffic consistent with the hydrodynamic theory. *Transp. Res., Part B* 28 (4), 269–287.
- David Schrank, B.E., Lomax, Tim, 2012. Annual Urban Mobility Report. Tech. rep., Texas Transportation Institute.
- Gomes, G., Horowitz, R., 2006. Optimal freeway ramp metering using the asymmetric cell transmission model. *Transp. Res. Part C* 14 (4), 244–262.
- Gomes, G., Horowitz, R., Kurzhanskiy, A.A., Varaiya, P., Kwon, J., 2008. Behavior of the cell transmission model and effectiveness of ramp metering. *Transp. Res. Part C: Emerg. Technol.* 16 (4), 485–513. <http://dx.doi.org/10.1016/j.trc.2007.10.005>, <<http://www.sciencedirect.com/science/article/pii/S0968090X0700085X>>.
- Hegyi, A., Schutter, B.D., Hellendoorn, H., 2005. Model predictive control for optimal coordination of ramp metering and variable speed limits. *Transp. Res. Part C: Emerg. Technol.* 13 (3), 185–209.
- Heydecker, B., Addison, J., 2010. Lane distribution of traffic near merging zones influence of variable speed limits. In: 13th International IEEE Conference on Intelligent Transportation Systems, pp. 485–490.
- Heydecker, B., Addison, J., 2011. Analysis and modelling of traffic flow under variable speed limits. *Transp. Res. Part C: Emerg. Technol.* 19 (2), 206–217.
- Jin, W.-L., 2010. A kinematic wave theory of lane-changing traffic flow. *Transp. Res. Part B: Methodol.* 44 (89), 1001–1021.
- Kotsialos, A., Papageorgiou, M., 2004. Nonlinear optimal control applied to coordinated ramp metering. *Control Syst. Technol., IEEE Trans.* 12 (6), 920–933.
- Kotsialos, A., Papageorgiou, M., Mangeas, M., Haj-Salem, H., 2002. Coordinated and integrated control of motorway networks via non-linear optimal control. *Transp. Res. Part C: Emerg. Technol.* 10 (1), 65–84.
- Leclercq, L., Laval, J.A., Chiabaut, N., 2011. Capacity drops at merges: an endogenous model. *Proc. – Soc. Behav. Sci.* 17 (0), 12–26, papers selected for the 19th International Symposium on Transportation and Traffic Theory. <http://dx.doi.org/10.1016/j.sbspro.2011.04.505>, <<http://www.sciencedirect.com/science/article/pii/S1877042811010640>>.
- Mosek. <<https://www.mosek.com/>> (accessed 3.21.2015).
- Muralidharan, A., 2012. Tools for Modeling and Control of Freeway Networks. Ph.D. Thesis, University of California, Berkeley.
- Muralidharan, A., Horowitz, R. Supporting material for computationally efficient model predictive control of freeway networks.
- Muralidharan, A., Horowitz, R., 2012. Optimal control of freeway networks based on the link node CTM. In: ACC Conference Proceedings.
- Muralidharan, A., Dervisoglu, G., Horowitz, R., 2009. Freeway traffic flow simulation using the cell transmission model. In: Proceedings of the American Control Conference, St. Louis, 2009.
- Muralidharan, A., Horowitz, R., Varaiya, P., 2012. Model predictive control of a freeway network with capacity drops. In: ASME DSCC Conference Proceedings.
- Papageorgiou, M., Mayr, R., 1982. Optimal decomposition methods applied to motorway traffic control. *Int. J. Control* 35, 269–280.
- Papageorgiou, M., Hadj-Salem, H., Blosseville, J., 1991. ALINEA: a local feedback control law for on-ramp metering. *Transp. Res. Rec.* 1320, 58–64.
- Papageorgiou, M., Hadj-Salem, H., Middleham, F., 1997. ALINEA local ramp metering: Summary of field results. *Transp. Res. Rec.* 1603, 90–98.
- Papageorgiou, M., Kosmatopoulos, E., Papamichail, I., 2008. Effects of variable speed limits on motorway traffic flow. *J. Transp. Res. Board* (3748) Transportation Research Record No 2047.
- Papamichail, I., Kotsialos, A., Margonis, I., Papageorgiou, M., 2010. Coordinated ramp metering for freeway networks – a model-predictive hierarchical control approach. *Transp. Res. Part C: Emerg. Technol.* 18 (3), 311–331.
- Papamichail, I., Papageorgiou, M., Vong, V., Gaffney, J., 2010. Heuristic ramp-metering coordination strategy implemented at Monash freeway, Australia. *Transp. Res.* 2178, 10–20.
- Smaragdis, E., Papageorgiou, M., 2003. A series of new local ramp metering strategies. *Transp. Res. Rec.* 1856, 7486.
- Sun, X., Horowitz, R., 2005. A localized switching ramp-metering controller with a queue length regulator for congested freeways. In: Proceedings American Control Conference, Portland, OR.
- van den Hoogen, E., Smulders, S., 1994. Control by variable speed signs: results of the dutch experiment. In: Road Traffic Monitoring and Control, 1994, Seventh International Conference on, pp. 145–149. doi:10.1049/cp:19940444.
- Wattleworth, J., 1965. Peak Period Analysis and Control of A Freeway System. Highway Research Record 157.
- Zhang, M., Kim, T., Nie, X., Jin, W., Chu, L., Recker, W., 2001. Evaluation of On-ramp Control Algorithms. Tech. rep. UCB-ITS-PRR-2001-36, California PATH.
- Ziliaskopoulos, A., 2000. A linear programming model for the single destination system optimum dynamic traffic assignment problem. *Transp. Sci.* 34-1, 37–49.